

SRI International

Quarterly Technical Report #13 (Revised) • November 1995

ADVANCED SEPARATION TECHNOLOGY FOR FLUE GAS CLEANUP

Abhoyjit S. Bhowm
Neeraj Pakala
Tracy Riggs
Troy Tagg

Kamalesh K. Sirkar
Sudipto Majumdar
Debabrata Bhaumick

SRI International
333 Ravenswood Avenue
Menlo Park, CA 94025

New Jersey Institute of Technology
University Heights
Newark, NJ 07102

SRI Project No. PYU-3501

Prepared for:

U.S. DEPARTMENT OF ENERGY
Pittsburgh Energy Technology Center
P.O. Box 10940
MS 921-118
Pittsburgh, PA 15236-0940

Attn: Document Control Center

DOE Contract No. DE-AC22-92PC91344

333 Ravenswood Avenue • Menlo Park, CA 94025-3493 • (415) 326-6200 • FAX: (415) 326-5512 • Telex: 334486

MASTER

DISTRIBUTION OF THIS DOCUMENT IS UNLIMITED

RECEIVED
JSDOE/PETC
65 NOV -6 AM 11:04
ASSISTANCE DIV.

CONTENTS

INTRODUCTION 1

SUMMARY OF QUARTERLY PROGRESS 3

TASK 8: INTEGRATED NO_x LIFE TESTS 4

TASK 9: PERFORMANCE OF SCALABLE MODULES..... 14

DISCLAIMER

This report was prepared as an account of work sponsored by an agency of the United States Government. Neither the United States Government nor any agency thereof, nor any of their employees, makes any warranty, express or implied, or assumes any legal liability or responsibility for the accuracy, completeness, or usefulness of any information, apparatus, product, or process disclosed, or represents that its use would not infringe privately owned rights. Reference herein to any specific commercial product, process, or service by trade name, trademark, manufacturer, or otherwise does not necessarily constitute or imply its endorsement, recommendation, or favoring by the United States Government or any agency thereof. The views and opinions of authors expressed herein do not necessarily state or reflect those of the United States Government or any agency thereof.

MASTER

FIGURES

1	Co(II)-Phalocyanine-Standard Curves.....	5
2	Modified NO _x Absorption and Desorption Experimental Arrangement.....	7
3.	Flow Calibration Curve.....	8
4.	Absorption and desorption Processes Exiting Gas NO Concentrations as a Function of Time.....	10
5.	NO _x Scrubbing Solution Lifetime Data.....	11
6.	NO _x Absorption/Desorption Experimental Setup (Enhanced Desorption Operation).....	13
7.	Drawing of Rectangular Housing.....	15
8.	Design Features of a Submodule.....	16
9.	Top-View of the Gas-Side End Plates of Housing.....	17
10.	SO ₂ Analyzer for Continuous Monitoring of Gas Streams.....	19
11.	Percent SO ₂ Removal Versus Water Flow Rate.....	21
12.	Percent SO ₂ Removal Versus Gas Flow Rate.....	22
13.	SO ₂ - Water Equilibrium Curves.....	23
14.	Mass Transfer Coefficient Versus Water Flow Rate.....	24
15.	Mass Transfer Coefficient Versus Gas Flow Rate.....	25

TABLES

1.	Project Tasks and Schedule	2
2.	Mass Flow Controllers (MFCs) and Settings.....	6

INTRODUCTION

The objective of this work is to develop a novel system for regenerable SO₂ and NO_x scrubbing of flue gas that focuses on (a) a novel method for regeneration of spent SO₂ scrubbing liquor and (b) novel chemistry for reversible absorption of NO_x. In addition, high efficiency hollow fiber contactors (HFC) are proposed as the devices for scrubbing the SO₂ and NO_x from the flue gas. The system will be designed to remove more than 95% of the SO_x and more than 75% of the NO_x from flue gases typical of pulverized coal-fired power plants at a cost that is at least 20% less than combined wet limestone scrubbing of SO_x and selective catalytic reduction of NO_x. In addition, the process will make only marketable byproducts, if any (no waste streams).

The major cost item in existing technology is capital investment. Therefore, our approach is to reduce the capital cost by using high efficiency hollow fiber devices for absorbing and desorbing the SO₂ and NO_x. We will also introduce new process chemistry to minimize traditionally well-known problems with SO₂ and NO_x absorption and desorption. For example, we will extract the SO₂ from the aqueous scrubbing liquor into an oligomer of dimethylaniline to avoid the problem of organic liquid losses in the regeneration of the organic liquid. Our novel chemistry for scrubbing NO_x will consist of water soluble phthalocyanine compounds invented by SRI and also of polymeric forms of Fe⁺⁺ complexes similar to traditional NO_x scrubbing media described in the open literature. Our past work with the phthalocyanine compounds, used as sensors for NO and NO₂ in flue gases, shows that these compounds bind NO and NO₂ reversibly and with no interference from O₂, CO₂, SO₂, or other components of flue gas.

The final novelty of our approach is the arrangement of the absorbers in cassette (stackable) form so that the NO_x absorber can be on top of the SO_x absorber. This arrangement is possible only because of the high efficiency of the hollow fiber scrubbing devices, as indicated by our preliminary laboratory data. This cassette (stacked) arrangement makes it possible for the SO₂ and NO_x scrubbing chambers to be separate without incurring the large ducting and gas pressure drop costs necessary if a second conventional absorber vessel were used. Because we have separate scrubbers, we will have separate liquor loops and deconvolute the chemical complexity of simultaneous SO₂/NO_x scrubbing.

We will conduct our work in a 60-month period (5/92 to 4/97), encompassing 16 tasks (Table 1), beginning with studies of the fundamental chemistry and of the mass transfer characteristics of small HFC modules in the laboratory. We will then examine the most favorable method of SO₂ liquor regeneration, determine the ability of the HFC devices to withstand particulate matter,

and examine the behavior of scalable modules. In the final 15 months of the program, we will determine the fundamental mass transfer behavior of a subscale prototype system. Based on these data, a computational design model will be devised to guide further scaleup efforts that may follow.

Table 1
PROJECT TASKS AND SCHEDULE

Task Number	Title	Duration
1	Project Definition	5/92 – 8/92
2	Capacity, Reversibility and Lifetime	7/92 – 6/94
3	Chemical Synthesis	7/92 – 6/94
4	SO ₂ Scrubbing with HFCs	7/92 – 9/93
5	NO _x Scrubbing with HFCs	2/93 – 3/94
6	SO ₂ Liquor Regeneration	7/93 – 9/94
7	Particle Deposition	8/93 – 9/94
8	Integrated NO _x Life Tests	8/94 – 1/96
9	Scalable Modules	9/94 – 1/96
10	Computational Model	3/95 – 1/96
11	Construction of Subscale Prototype	2/96 – 4/96
12	Operation of Subscale Prototype	5/96 – 4/97
13	Refinement of Computational Model	1/97 – 4/97
14	Economic Evaluation	Various
15	Reporting	5/92 – 4/97
16	Chemical Synthesis for Process Scale-up	5/94 – 4/96

SUMMARY OF QUARTERLY PROGRESS

During the second quarter of 1995, we continued work on Task 8. We also obtained some mass transfer data on Task 9.

In Task 8, we have presented the modified experimental arrangement for testing the efficacy of Co(II)-phthalocyanine solution for NO_x absorption as well as desorption over extended periods of time. This arrangement allows us to automatically acquire data and control process parameters. We obtained absorption/desorption data over a period of 140 hours. The data exhibits average NO removal rates of 50%. In order to increase the overall efficiency of the system, we have designed and built a new desorption section with increased mass transfer area.

In Task 9, we presented the design details of the rectangular scalable modules. Also, we tested the apparatus with SO₂/water system. The performance of the device was affected by varying either gas or water flow rates. SO₂ removal rates close to 90% were obtained at 20 SLPM gas flow rates.

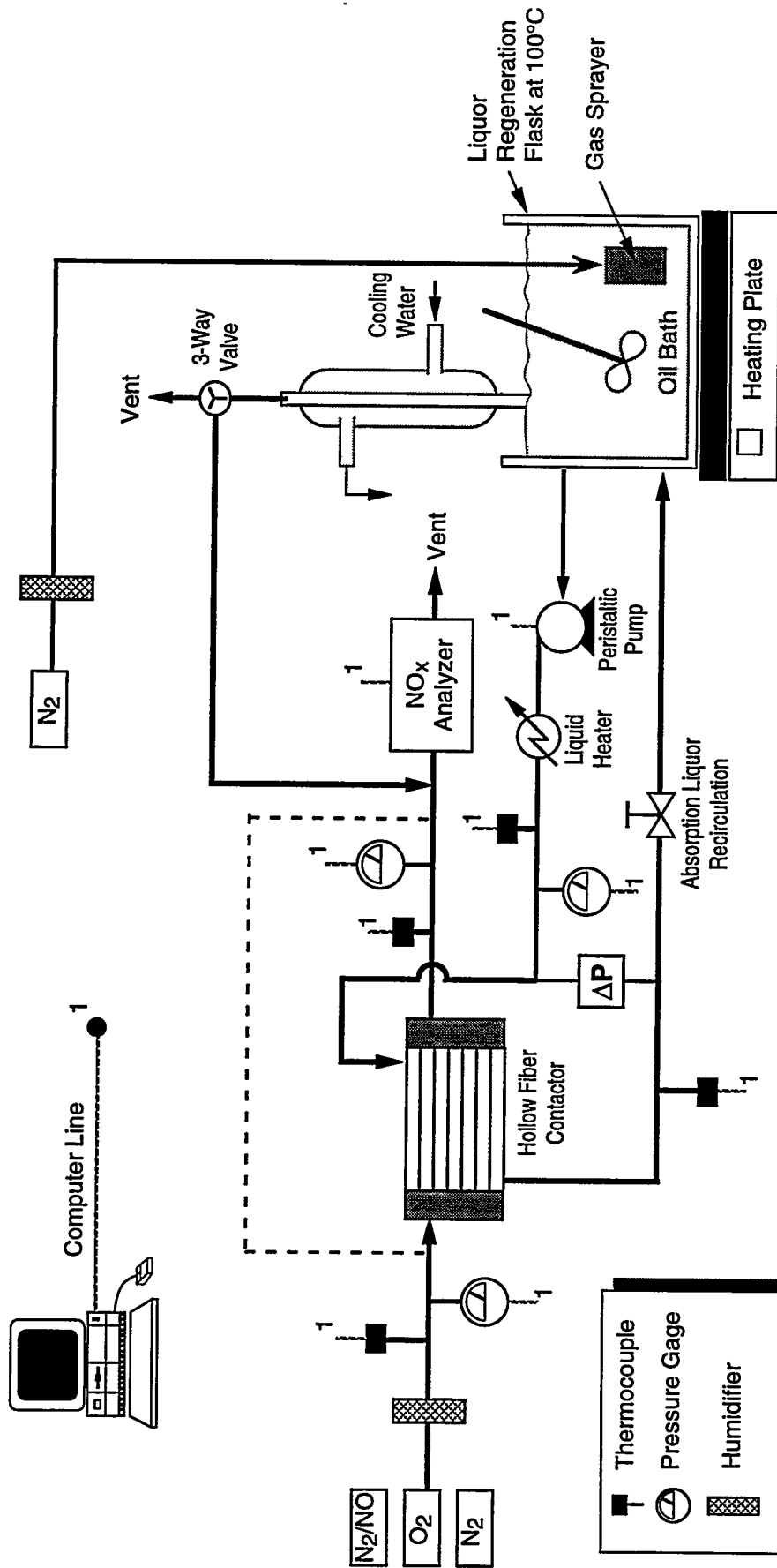
TASK 8: INTEGRATED NO_x LIFE TESTS

Liquid scrubbing systems for NO_x have traditionally been plagued by degradation of performance over time with subsequent need for convoluted liquor regeneration schemes. Therefore, it is essential to determine whether or to what extent there is any loss with time in the performance of the NO_x absorption/desorption system. We have previously shown that Co(II)-phthalocyanine is a promising candidate for NO_x absorption in the presence of O₂. We have also demonstrated the superior mass transfer characteristics of the Co(II)-phthalocyanine scrubbing system in a 300 fiber HFC. Consequently, the objective here is to devise a continuously operating system for determining if the NO_x absorption/desorption chemistry has the potential to be commercially robust.

Initial experiments have shown that over a short period of time (40 hr.) no deactivation of Co(II)-phthalocyanine occurred (Quarterly Technical Report #11). In order to carry out these long term experiments with greater efficiency, the apparatus has been set up for automatic data acquisition and control. During the beginning of this quarter, our efforts are directed towards testing the various equipment and the data acquisition capabilities.

In December 1994, we reported that the NO_x analyzer was not giving a constant reading over time for a given calibration gas—the analyzer would slowly yet significantly drift upward. The unit was sent to the manufacturer for repair. We tested the analyzer to make sure it is in working condition. A calibration gas (Liquid Carbonic, Menlo Park, CA) of 480 ppm NO was used to calibrate the unit. A second calibration gas of 48 ppm was used to test the consistency of the unit. A reading of 46 ppm was obtained; about a 4% error. Given that the range of the first calibration gas is ten times greater than that of the second, the error is acceptable. For all the experiments, the unit will be calibrated using the 48 ppm standard cylinder, since this is in the near vicinity of the expected concentrations from the process. However, we also plan to test the calibration of the system using both cylinders (48 and 480 ppm NO in N₂) quite frequently.

A system has been designed and built to test the absorption and desorption behavior of solutions over extended periods of time. Figure 1 is a schematic of this system. It is interfaced with a computer for automatic data acquisition and control. The system includes six mass flow controllers that were calibrated to give the desired flow. Table 2 shows the function, desired flow, and required setting for each controller.



CM-360583-32E

Figure 1. Modified NO_x absorption and desorption experimental arrangement.

Table 2. Mass Flow Controllers (MFC) and Settings.

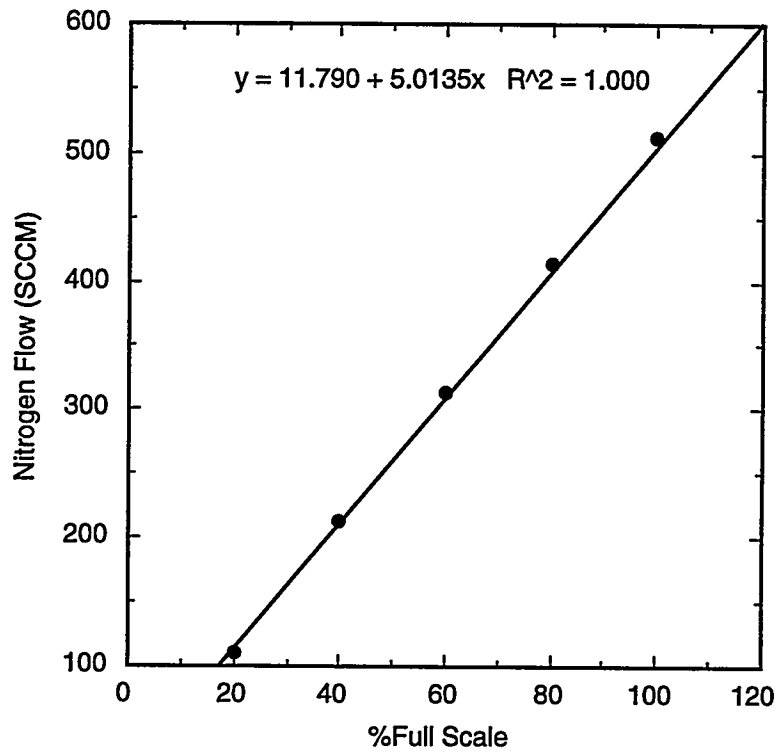
MFC Number	Function	Type of Gas Used	Desired Flow	Required Setting
1	NO Feed	1% NO in N ₂	4.9 SCCM	4.4 SCCM
2	N ₂ Feed	Nitrogen	90.6 SCCM	84.2 SCCM
3	O ₂ Feed	Oxygen	4.5 SCCM	16.5% FS
4	Make-up Stream	Nitrogen	500 SCCM	94.7% FS
5	Make-up Stream	Nitrogen	100 or 300 SCCM	24.9% or 82.7% FS
6	Stripping Gas	Nitrogen	300 SCCM	283 SCCM

As given in Table 2, MFC #5 has 2 desired settings. This is because the NO_x analyzer requires a constant flow of 900 SCCM. When the exit stream from the absorber (100 SCCM) is analyzed, a make-up gas flow of 800 SCCM is required. This is achieved by MFC #4 in parallel with MFC #5 set in the 300 SCCM mode. When, on the other hand, the stream from the desorber (MFC #6 at 300 SCCM) is analyzed, a make-up gas flow of 600 SCCM is obtained by MFC #4 in parallel with MFC #5 set in the 100 SCCM mode. Figure 2 is a representative calibration curve for MFC #5.

We developed a method to determine the concentration of Co(II)-phthalocyanine in scrubbing solution. Standard solutions at different concentrations were prepared and analyzed on a UV spectrophotometer. Appropriate absorption peaks were determined (based on the standards) to be at 218 nm and 320 nm wavelengths. A standard curve for each wavelength was plotted and shown to have excellent linearity (Figure 3). Therefore, these standard curves were used to analyze unspent scrubbing solution as discussed below.

The UV spectrophotometer method consists of obtaining a small sample (about 400 μ L) of solution and diluting it with water to obtain 1 Liter total solution. A portion of the diluted sample is analyzed on an Hewlett Packard 8452A Diode Array Spectrophotometer. The absorbance at 218 nm and 320 nm is recorded and compared to a known standard curve. The prepared solution for the experiment was determined to be about 95 mM Co(II)-phthalocyanine. The solution inside the contactor, however was determined to be about 75 mM. This discrepancy is due to a small volume of water remained in the contactor due to our initial leak tests with water.

On May 16, 1995, we began the first run using NO and the Co(II)-phthalocyanine solution. The exit stream from the absorber was monitored for NO content. Initially, the readings were around 2-3 ppm, which was expected. The reading did not increase, however, for several hours.



CM-3501-101

Figure 2. Flow calibration curve.

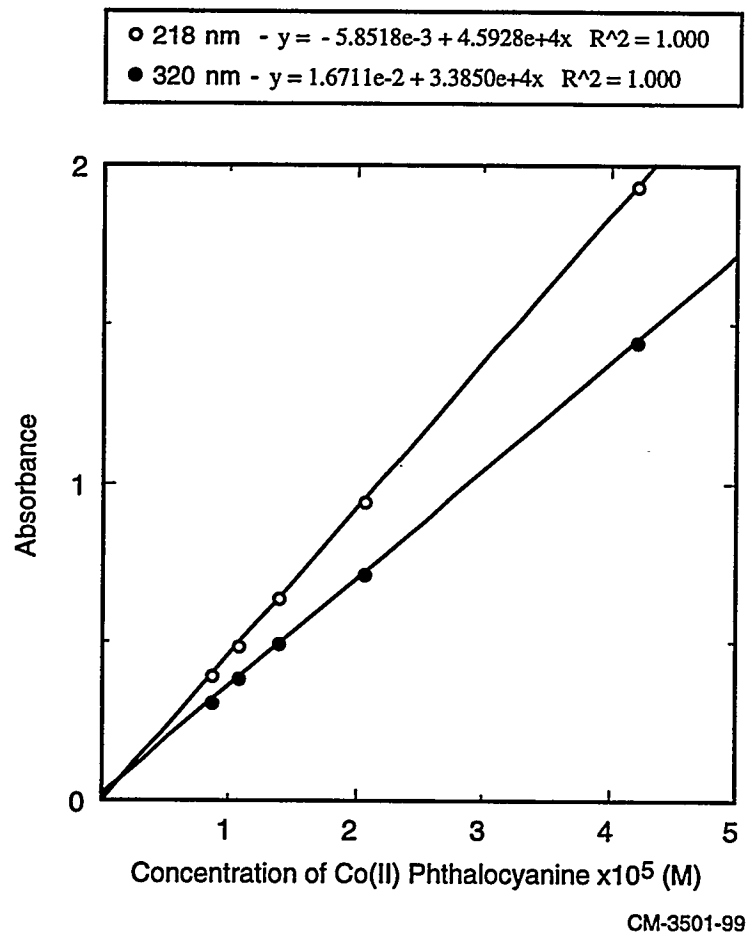


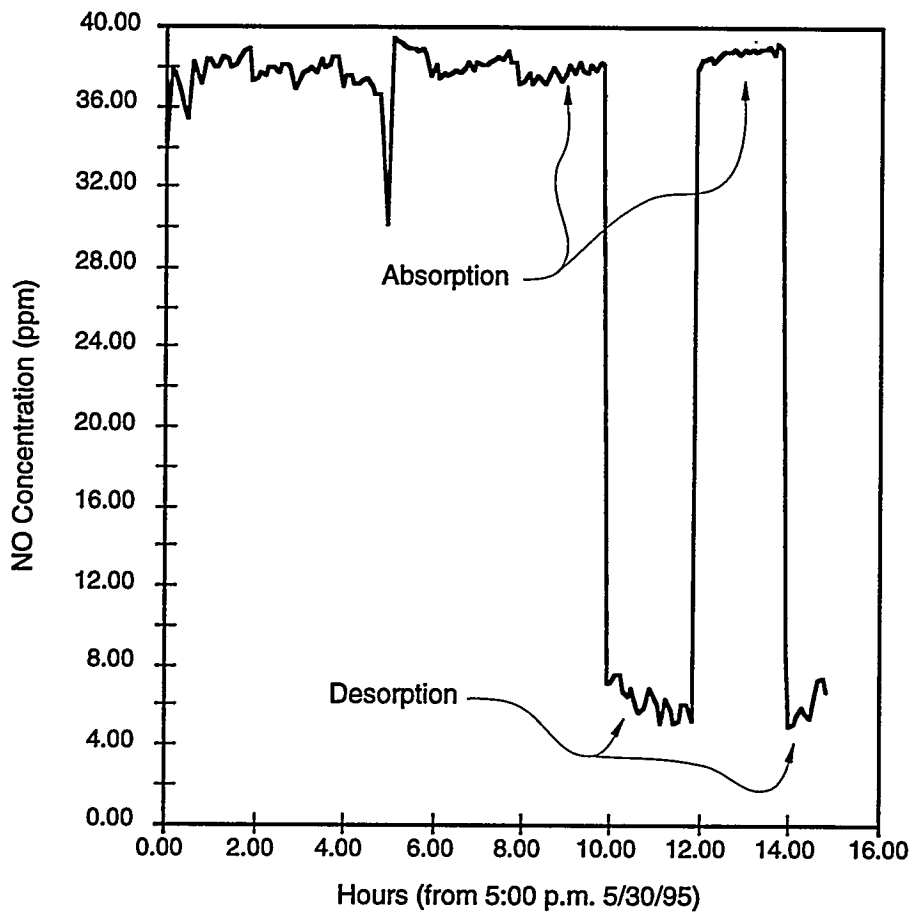
Figure 3. Co(II) phthalocyanine - standard curves.

At this point we thought that because of the large volume of liquid (about 450 ml) and the dilute (500 ppm NO and 100 SCCM) feed stream, the system would take an exceedingly long period of time to reach steady state. We decided to increase the feed concentration to 1800 ppm NO. The system was run in this configuration overnight. The exit gas from the desorber the next morning showed only 10 ppm NO. A simple calculation showed that the system was still not at steady state (mass balance closure was only about 30%), yet the concentration of the exit stream from the absorber was fairly constant over a 16 hr. period (about 11-12 ppm). In order to check the gas leaks in plumbing, we decided to shunt the gas side of the HFC. This exercise revealed no such problem. After placing the contactor back in line, however, the behavior of the system changed. The exit stream from the absorber was about 1350 ppm (feed is 1800 ppm) while the exit after the desorber was about 30 ppm. Encouraged at this change, we set the feed back down to 500 ppm NO and let the system run for about 15 hrs (total time now logged by the liquid is about 126 hrs). As seen in Figure 4, the absorption and desorption characteristics are completely opposite of what is expected. It is expected that at a steady state, the exit gas stream after absorption would contain only about 20-30% of the NO in the feed. For this test, about 70% of the NO in the feed was noticed after the absorber. Furthermore, the mass balance closure was only about 80%.

Either the absorber/plumbing system is faulty (including leaks, plugged fibers, etc.) or the liquor is completely saturated with NO. The former seems more plausible than the latter because previous tests of about 40 hrs showed that no degradation of the Co(II)-phthalocyanine solution occurred (Quarterly Technical Report #11).

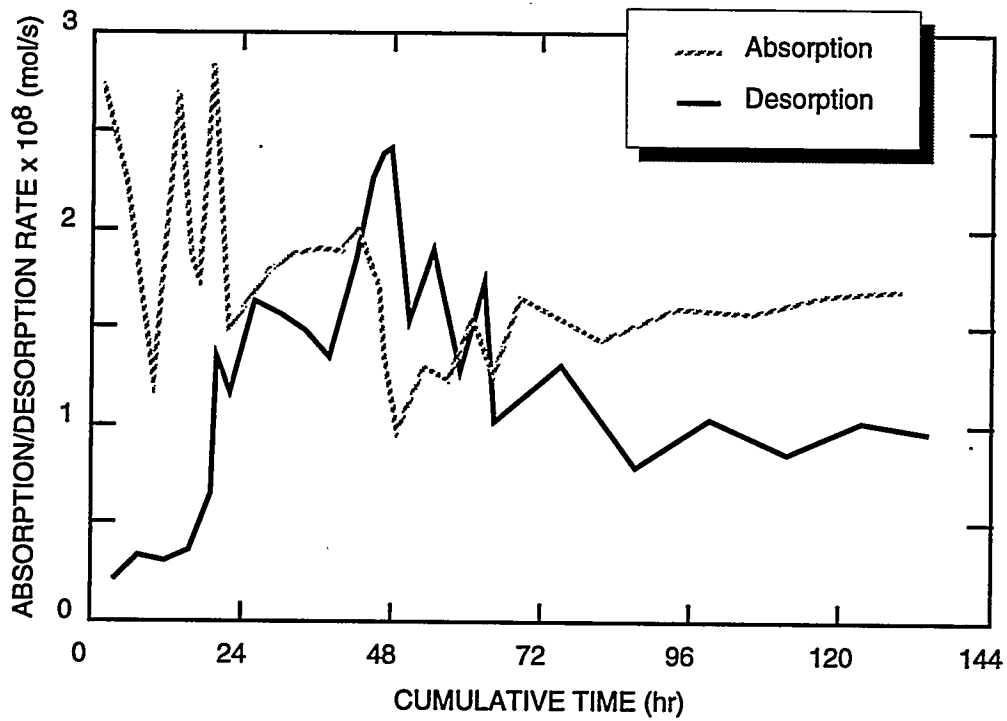
During the end of this reporting period, in an attempt to close the mass balance between absorption and desorption processes, we tried using a simple glass flask in place of HFC and sparging NO gas stream through the scrubbing liquid (water) contained in the flask. This operation posed serious difficulties in maintaining constant amount of liquid in the flasks. This is because the gas and liquid are directly in contact with one another (unlike HFC operation) and therefore the recirculation (flow) of liquid between absorption and desorption flasks was depended on several factors: one, the pressure differential generated by peristaltic pump, two, the pressure of gas contained in head space of each flask and, three, the gravitational pressure head. Therefore, we could not maintain the flow between the processes. However, thorough cleaning and testing of the HFC seemed to solve the problem, as the mass balance of the system approached close after several hours of operation.

We obtained data for a period of about 140 hours (cumulative time logged on the scrubbing liquor). Figure 5 shows absorption/desorption characteristics of the liquid over this time. As expected, during the starting period, the absorption rate is complete (100%) and the desorption rate is zero. By the end of the second day of the operation, both absorption and desorption rates



CM-3501-100

Figure 4. Absorption and desorption processes exiting gas NO concentrations as a function of time.

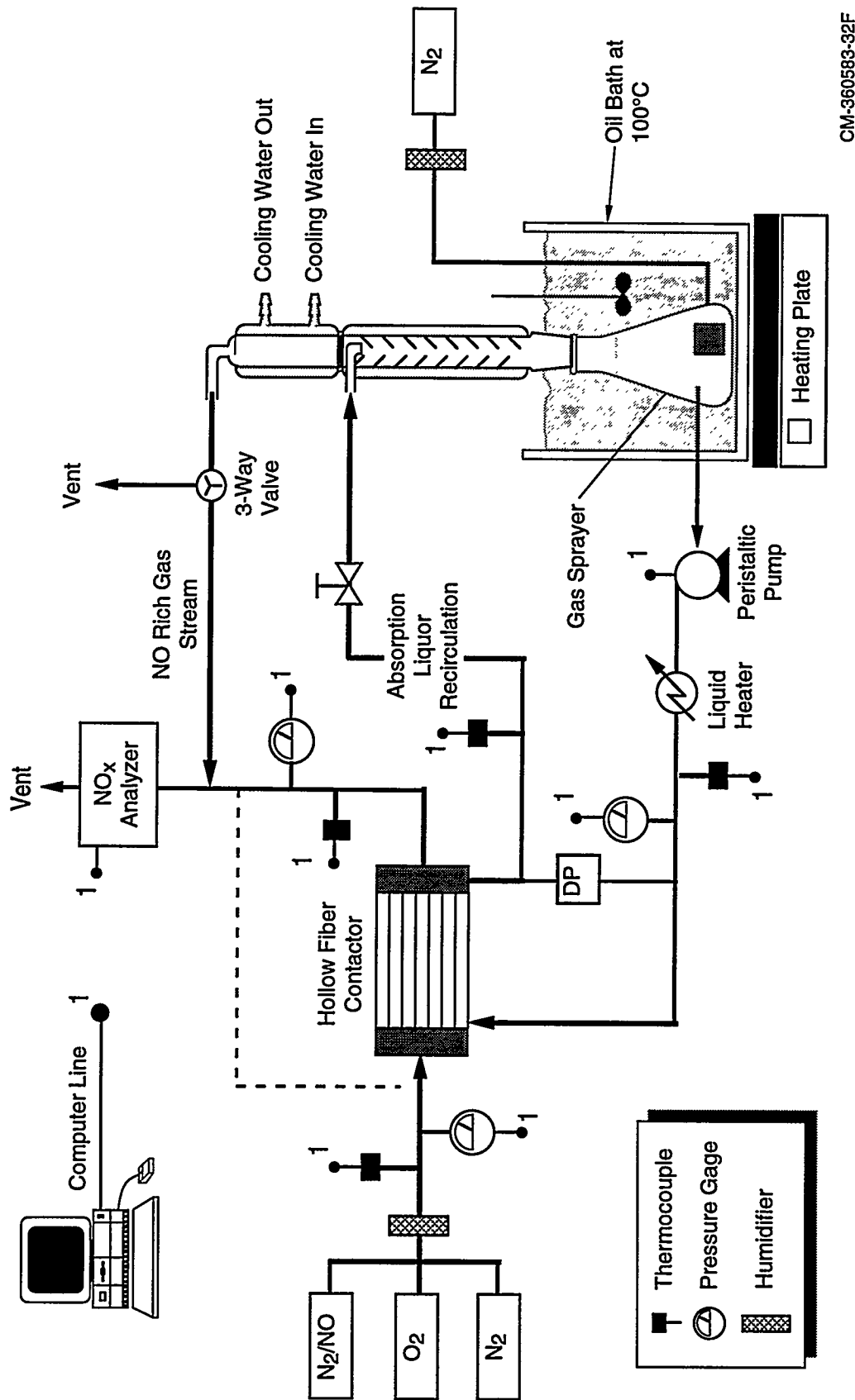


CM-3501-102

Figure 5. NO_x scrubbing solution lifetime data.

became stabilized. From the data shown, the average NO removal rate calculated as 50%. However, in Task 5 (Quarterly Technical Report #9) 85% NO removal rates were demonstrated using the same 300 fiber HFC. Therefore, we believe that the desorption process is limiting the overall efficiency of the system.

In order to increase the efficiency of the desorber, the operation is made countercurrent and the mass transfer area is increased with help of baffles. Figure 6 is a schematic of this arrangement. The stripping section has a condenser affixed at the top which is filled with glass beads. The glass beads are supported by a fritted glass barrier, allowing gas to flow up, and liquid to flow down. Shortly after fabrication and installation of the stripping section, we experienced difficulties in calibrating NO_x analyzer due to some scrubbing liquid entrained into the equipment. We hope to resolve the problem by simply dismantling and cleaning the affected parts.



CM-360583-32F

Figure 6. NO_x absorption/desorption experimental setup (enhanced desorption operation).

TASK 9: PERFORMANCE OF SCALABLE MODULES

Because of the need for billions of (approximately 30-cm long) fibers to treat the flue gas from a 500 MW(e) plant, it is critical to establish the mass transfer characteristics of a module that can be scaled up to a prototypical size. To appreciate this point, one must recognize that approximately 250,000 modules of 2" diameter would be required to provide one billion fibers. Such an arrangement would provide a ducting, plumbing, and maintenance nightmare in a full-scale plant and clearly would not be economical or workable. A new design concept, such as rectangular modules, is needed for a full-scale plant. Therefore, the objective of Task 9 is to develop the mass transfer fundamentals of rectangular modules.

The term "scalable module" is an important concept because it influences our ability to think about an eventual application of HFC devices to a 500 MW(e) power plant. We use the term to mean a module that exhibits the important phenomena that would appear in modules of the 500 MW(e) plant. For example, mass transfer in the rectangular (square) module will be different than that in the cylindrical modules because the flow pattern in a large-scale rectangular module absorber or liquid-liquid extractor will be crossflow, not countercurrent. Probably more importantly, flow distribution and liquid pressure drop behavior will be much different in a large "scalable" module than in our laboratory modules. Therefore, Task 9 is designed to obtain the fundamental mass transfer behavior, including issues of flow distribution and pressure drop, on modules that reflect these basic features of large-scale modules with gas and liquid flow rates in the range of 5-10 cfm and 1-5 l/min respectively.

At the beginning of this quarter, we received one of the rectangular hollow fiber contactors from Setec, Inc., Livermore, CA. The design details are discussed next.

The dimensions of the housing are 13.5" x 7.75" x 2.75" (Figure 7). The housing is designed to hold four 'submodules' each with dimensions 12.5" x 1.5" x 1.25". Figure 8 illustrates the design features of one submodule. The submodule contains 700 microporous polypropylene fibers, each with a length of 12", an outside diameter of 1 mm, an inner diameter of 0.6 mm, and a pore size of about 0.2 μm . At fiber ends, a cap is designed (see Figure 9 for side and top view of the cap) to uniformly collect the gas stream to each submodule. At the center of the plate, gas enters through 3/8" port and flows into a manifold that runs along the width (7.75" side) of the housing and allows the gas to flow into four 1/16" orifices, each one leading in a submodule. Thus the pressure drop across the orifices ensures uniform flow distribution amongst all four units. In addition, a 0.25" porex (sintered) material is used at the gas inlet of each submodule to equally distribute the gas stream into the fiber bundle. The gas outlet of the housing is designed exactly the same as the inlet, with the exception being that there is no porex material inside the submodule. The material of the housing is polycarbonate.

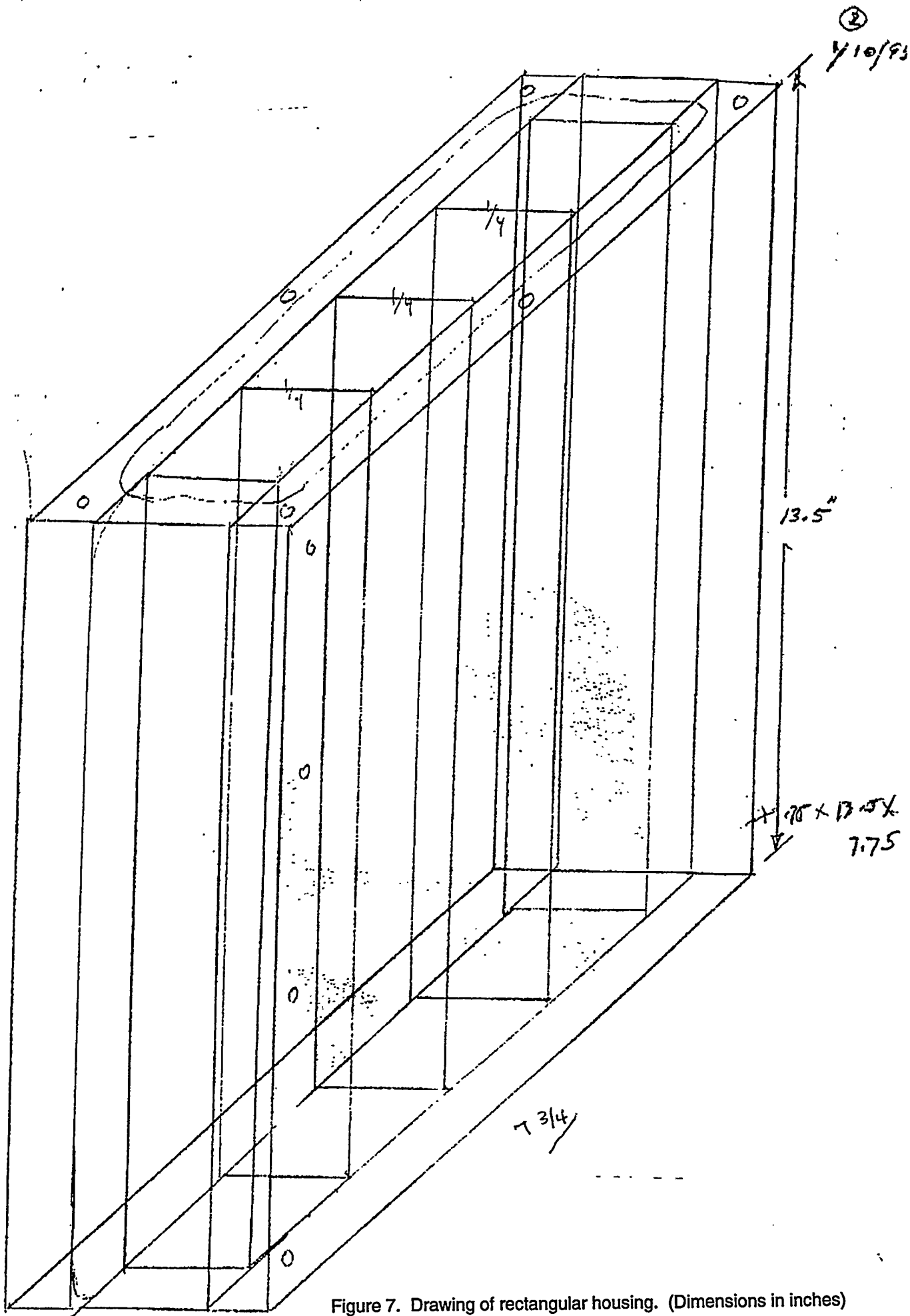


Figure 7. Drawing of rectangular housing. (Dimensions in inches)

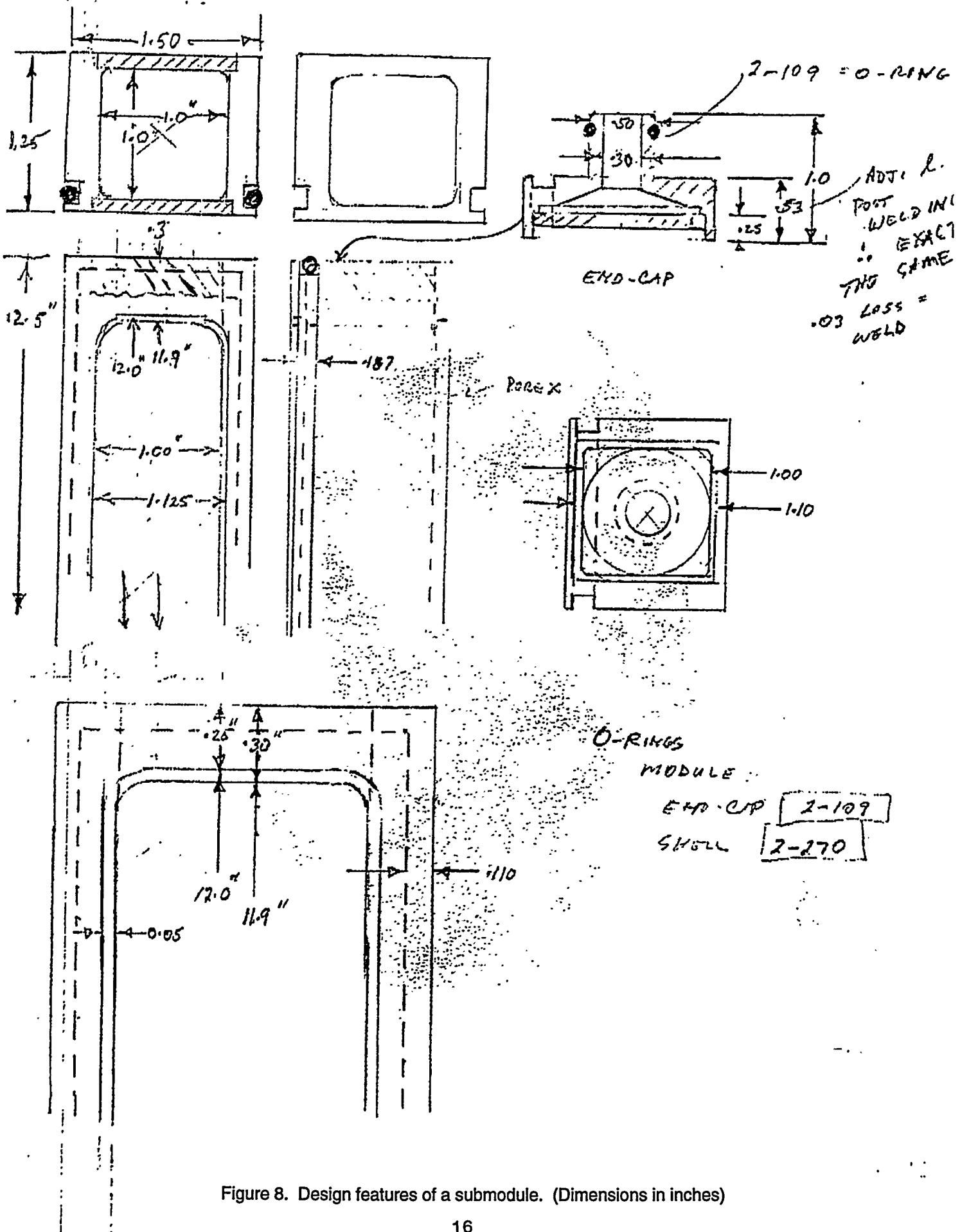
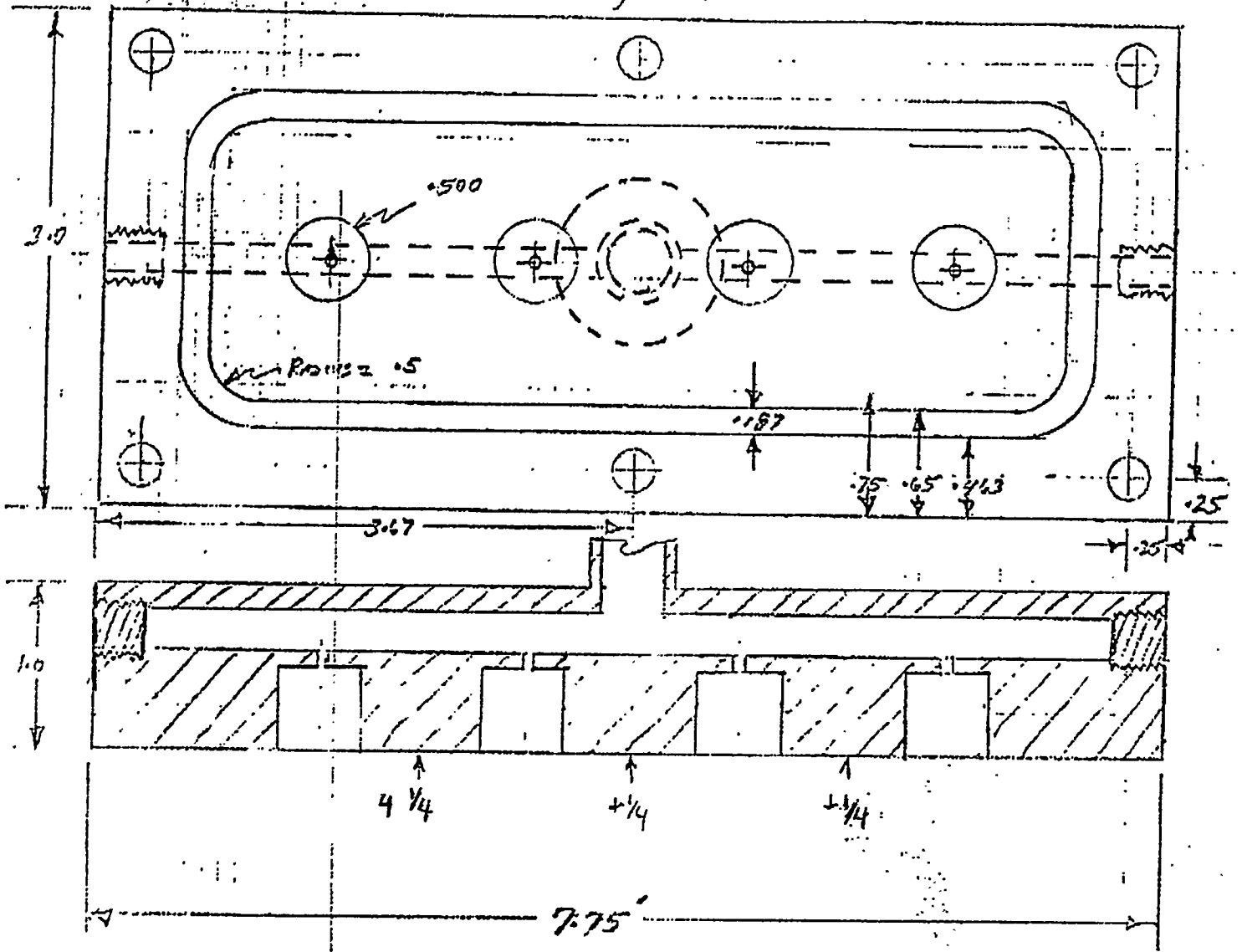


Figure 8. Design features of a submodule. (Dimensions in inches)

POLY CARBONATE HOUSING

④ 1/14

TOP/BOTTOM



alcohol
Phase
83 PS1

Figure 9. Top-view of the gas-side and plates of housing. (Dimensions in inches)

The liquid side of the housing is designed similar to the gas side, also with a manifold at the inlet that runs along the length of the module and separates the flow into twelve 1/16" orifices. There is a 12" x 1" piece of porex on the inlet side of each submodule, and a polycarbonate slab on the outlet containing about 36 orifices (approximately 1/8-inch diameter) for the liquid to flow out of and then into the porex of the next subunit. The liquid outlet of the housing is designed the same way as the inlet.

Before completing the fabrication of housing and submodules, we were supplied with a "tester" submodule which enabled us to measure the pressure drop across length of the fibers at various air flow rates. The results showed that we can flow up to 35 SLPM of air through the unit without exceeding the maximum pressure drop desired (10" water). Therefore, it is possible to treat 140 SLPM using all four submodules.

Upon receipt of the housing and all four submodules, we began testing the module using filtered water and filtered air. We encountered some problems with the housing; the ports on all four sides were unstable and broke off several times, and water leakage was occurring at some places in end plate joints. Therefore, we have sent the housing back to Setec to fix these problems.

During the meantime, we have acquired Model 40B SO₂ analyzer from Thermoenvironmental, Inc., Franklin, MA, through our internal resources. A schematic of the equipment is given in Figure 10. The analyzer detects SO₂ based on pulsed UV-fluorescence. This equipment is used as a continuous monitoring system with a sample gas flow rate of about 1 SLPM.

During the middle of the quarter, we received the rectangular module which was undergoing repairs at Setec. After testing again with air and water, the only problem we have encountered is a small water leak at one corner of the housing, which cannot be corrected unless the housing is rebuilt. The leak produces only about one drop every ten minutes, which is negligible compared to the liquid flow rates of about 1-5 L/min.

We conducted an experiment with 100 SLPM gas flow rate. The SO₂ concentration in the feed gas was 3000 ppm. The liquid (pure water) flow rate is maintained at 4.2 L/min. The SO₂ removal rate was measured to be 50%. At this point, the flow rates are somewhat limited by pressure drop. Although we believe the gas pressure drop through the fibers to be less than 10" of water at a flow rate of 100 SLPM (see the "tester" submodule data above), we can only measure the differential pressure across the entire housing, including the orifices and the porex material, which is about 5 psi. Similarly, we have noticed pressure drops on the liquid side of about 11-12 psi for a flow rate of 5 L/min. Because the transmembrane pressure should not exceed 22 psi, we

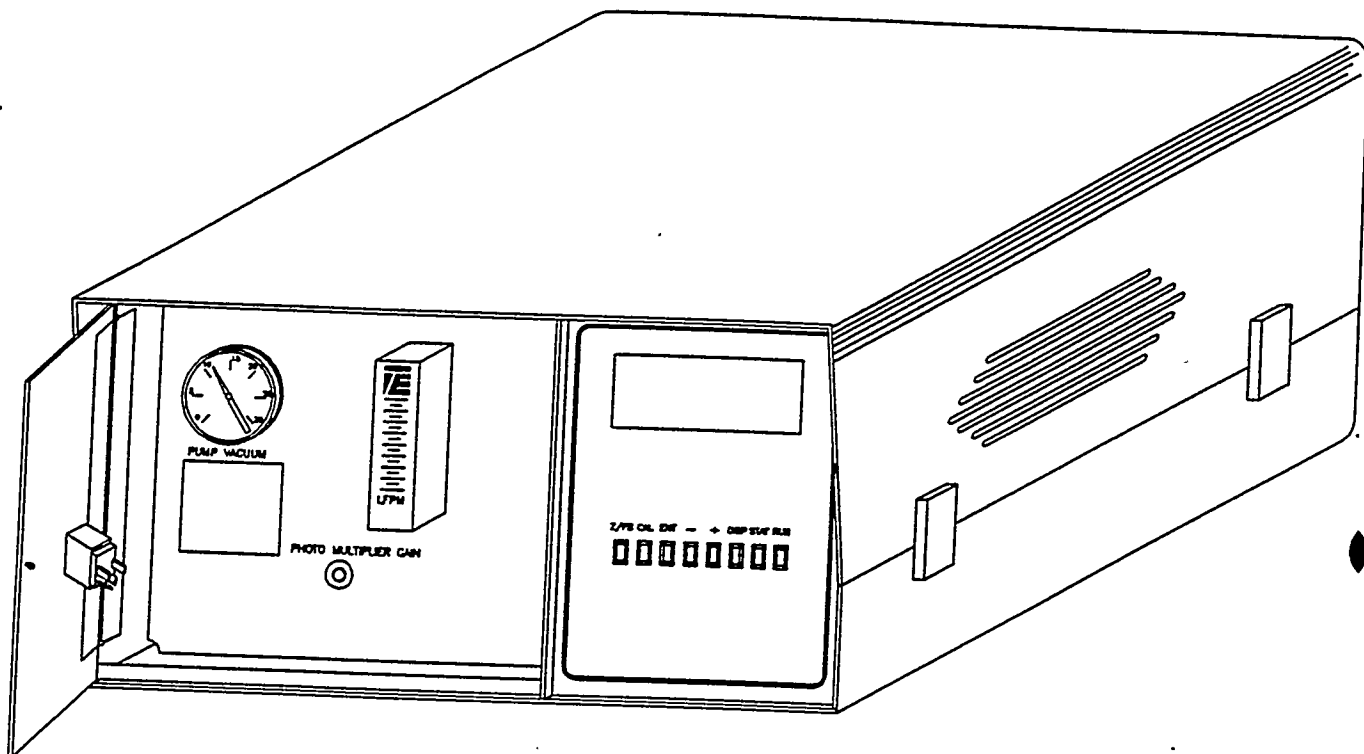


Figure 10. SO₂ Analyzer for continuous monitoring of gas streams.

are somewhat restricted on using higher flow rates of liquid. We may be able to solve this problem by increasing the size of the orifices (particularly those at the outlet, which are not really necessary for flow distribution).

During later stages of the quarter, we tested the rectangular module using pure water as the scrubbing liquid for SO₂ removal. The results of these experiments are summarized next.

The first set of experiments was conducted using a constant gas flow rate of 100 SLPM and varying water flow rates from 0.6 to 5 L/min. The SO₂ concentration in the feed gas was 3000 ppm. Figure 11 shows the percent of SO₂ removed as a function of water flow rate. In the second set of experiments, the liquid flow rate was held constant at 4.2 L/min, while the gas flow rate (still at 3000 ppm) was varied between 20 and 100 L/min. The removal results obtained for the various gas flow rates are shown in Figure 12. The highest SO₂ removal, about 85%, was obtained with a gas flow rate of 20 L/min and a liquid flow rate of 4.2 L/min.

The mass transfer coefficients for these experiments were calculated as follows,

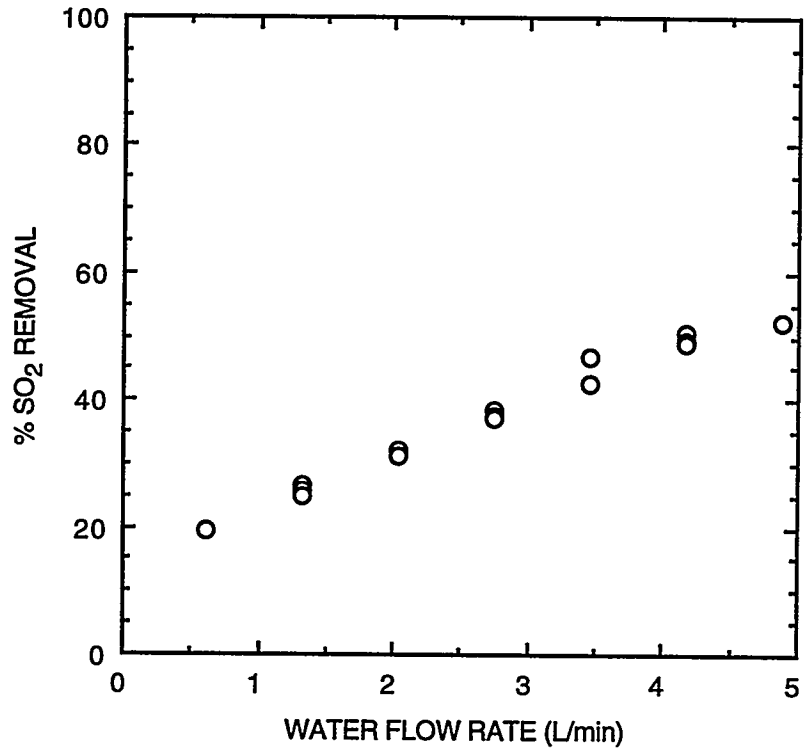
$$K_{og} = \frac{J_{SO_2}RT}{\Delta p_{lm}}$$

where K_{og} is the overall mass transfer coefficient in cm/s, J_{SO_2} is the flux of SO₂ across the membrane in mol/sec-cm², R is the gas-law constant, T is the temperature in Kelvins, and Δp_{lm} is the log-mean partial pressure difference in atm. The calculations were based on countercurrent flow, and therefore the log-mean difference was defined as

$$\Delta p_{lm} = \frac{(p_{in} - Hx_{out}) - (p_{out} - Hx_{in})}{\ln \left[\frac{(p_{in} - Hx_{out})}{(p_{out} - Hx_{in})} \right]}$$

where p_{in} is the partial pressure of SO₂ in the gas stream entering the contactor, p_{out} is the partial pressure of SO₂ in the exiting gas, x_{in} is the mole fraction of SO₂ in the entering liquid, x_{out} is the mole fraction of SO₂ in the exiting liquid, and H is Henry's law constant for the SO₂-water system in atm/mole fraction. The value for Henry's constant was determined to be 9596 mm Hg/mole fraction (12.6 atm/mole fraction) at 23° C from the equilibrium data shown in Figure 13 [Geankoplis, Christie, *Transport Processes and Unit Operations*. Allyn and Bacon, MA (1978)].

The calculated overall mass transfer coefficients as a function of the water flow rate and of the gas flow rate are shown in Figures 14 and 15, respectively. The graphs show that both the water flow and gas flow have an effect on the mass transfer coefficient.



CAM-3501-105

Figure 11. Percent SO₂ removal versus water flow rate.

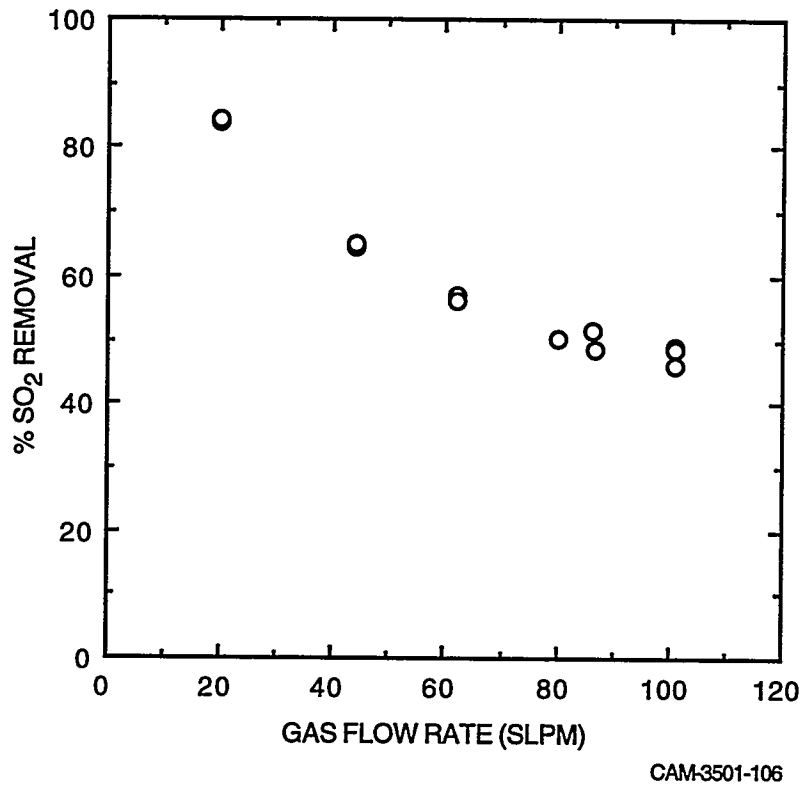
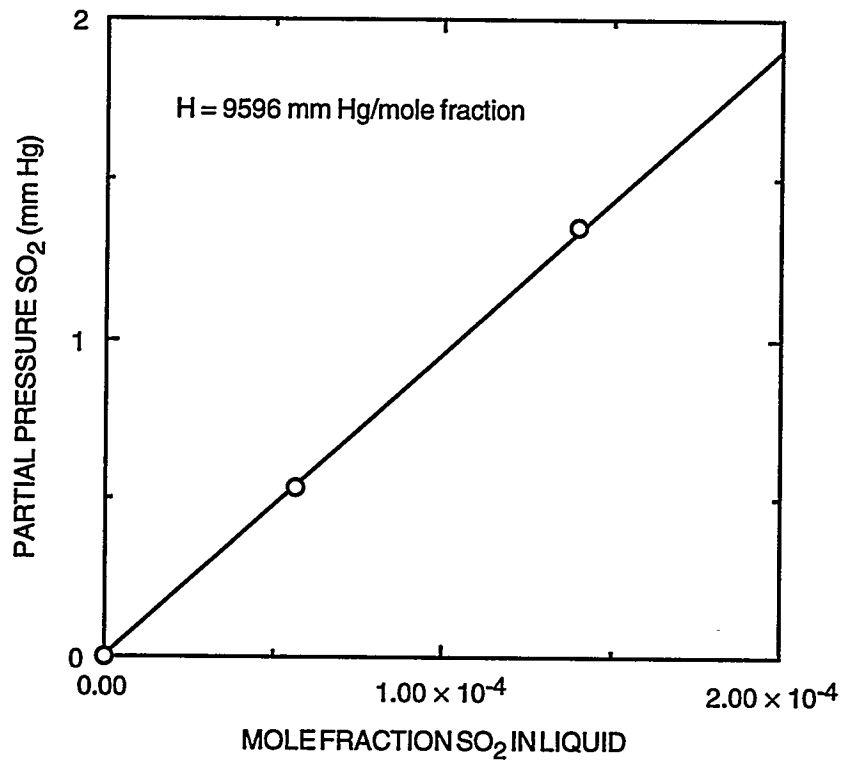
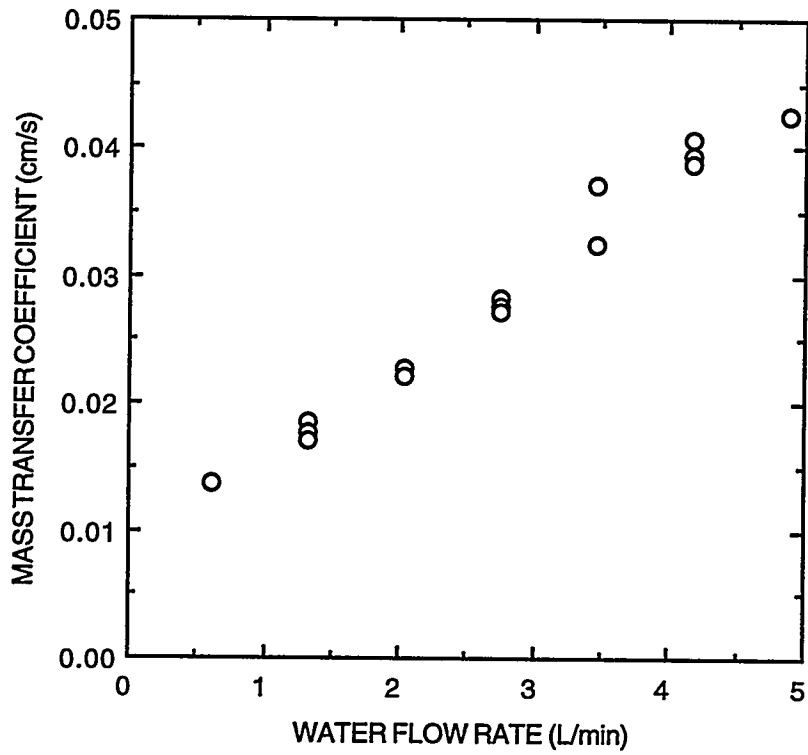


Figure 12. Percent SO₂ removal versus gas flow rate.



CAM-3501-107

Figure 13. SO₂-water equilibrium curve.



CAM-3501-108

Figure 14. Mass transfer coefficient versus water flow rate.

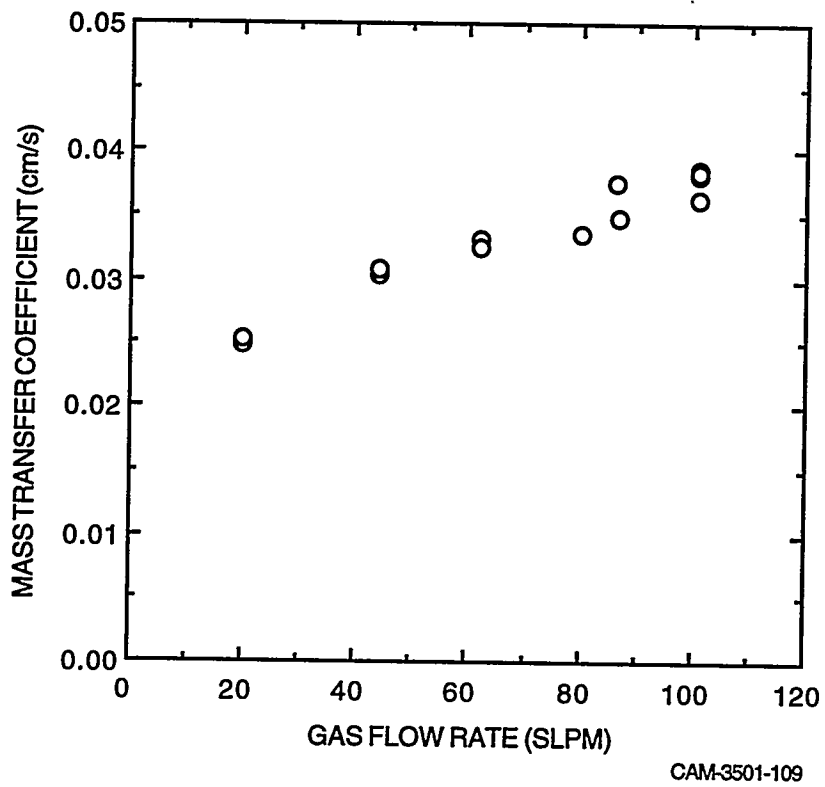


Figure 15. Mass transfer coefficient versus gas flow rate.